

RESEARCH ARTICLE

The recent normalization of historical marine heat extremes

Kisei R. Tanaka^{1*}, Kyle S. Van Houtan^{1,2*}

1 Monterey Bay Aquarium, Monterey, California, United States of America, **2** Nicholas School of the Environment, Duke University, Durham, North Carolina, United States of America

* kisei.tanaka@gmail.com (KRT); kyle.vanhoutan@gmail.com (KSVH)



OPEN ACCESS

Citation: Tanaka KR, Van Houtan KS (2022) The recent normalization of historical marine heat extremes. *PLoS Clim* 1(2): e0000007. <https://doi.org/10.1371/journal.pclm.0000007>

Editor: Maite deCastro, University of Vigo, SPAIN

Received: June 18, 2021

Accepted: November 8, 2021

Published: February 1, 2022

Copyright: This is an open access article, free of all copyright, and may be freely reproduced, distributed, transmitted, modified, built upon, or otherwise used by anyone for any lawful purpose. The work is made available under the [Creative Commons CC0](https://creativecommons.org/licenses/by/4.0/) public domain dedication.

Data Availability Statement: All data and scripts in this study are available at Github (<https://bit.ly/2QjhYld>) and through the Open Science Framework (<https://osf.io/mj8u7/>).

Funding: This study was supported by the generous contributions of members, visitors, and donors to the Monterey Bay Aquarium. The funders had no role in study design, data collection and analysis, decision to publish, or preparation of the manuscript.

Competing interests: The authors declare no competing interests.

Abstract

Climate change exposes marine ecosystems to extreme conditions with increasing frequency. Capitalizing on the global reconstruction of sea surface temperature (SST) records from 1870–present, we present a centennial-scale index of extreme marine heat within a coherent and comparable statistical framework. A spatially ($1^\circ \times 1^\circ$) and temporally (monthly) resolved index of the normalized historical extreme marine heat events was expressed as a fraction of a year that exceeds a locally determined, monthly varying 98th percentile of SST gradients derived from the first 50 years of climatological records (1870–1919). For the year 2019, our index reports that 57% of the global ocean surface recorded extreme heat, which was comparatively rare (approximately 2%) during the period of the second industrial revolution. Significant increases in the extent of extreme marine events over the past century resulted in many local climates to have shifted out of their historical SST bounds across many economically and ecologically important marine regions. For the global ocean, 2014 was the first year to exceed the 50% threshold of extreme heat thereby becoming “normal”, with the South Atlantic (1998) and Indian (2007) basins crossing this barrier earlier. By focusing on heat extremes, we provide an alternative framework that may help better contextualize the dramatic changes currently occurring in marine systems.

Introduction

The United States (US) National Oceanic and Atmospheric Administration (NOAA) generates the US Climate Normals [1] based on decadal averages of temperature and precipitation captured in the most recent climatological period. While the US Climate Normals provide advice for what may occur locally in the near future, fixed historical benchmarks may be more useful for describing contemporary climate departures and ecosystem disruptions. Such reference points are timely, as the persistent warming of sea surface temperatures (SST) and the increased frequency and intensity of extreme climatic events has fueled the perception that unprecedented climate normals are emerging in the global ocean [2, 3]. When it comes to measuring extremes, a large-scale shift in the mean and amplitude of ocean warming variability can affect the frequency of extreme temperature events through changes in the standard deviations and skewness [4, 5]. Nonetheless, increases in the frequency, magnitude, and

persistence of extreme marine heat events (variously defined) and climate disruptions have been recently described across spatiotemporal scales [6, 7].

Significant attention has been devoted to the detection and attributions of extreme marine heat events under observed and simulated climate variability (e.g., [5, 8, 9]). Hobday et al. [10] developed a framework to quantify the frequency and severity of marine heatwaves (MHWs), while Oliver et al. [11] analyzed longer time series and revealed centennial-scale increases in MHW properties. These new statistical frameworks provide a flexible definition of extreme marine heat events based on locally-defined fixed or sliding baselines and a seasonally varying threshold (e.g., 90th) applicable at many spatial and temporal scales [10, 12]. Drivers of extreme marine heat events include air-sea heat fluxes and horizontal temperature advection due to changes in ocean circulations [13–15]. The frequency and duration of MHWs have increased significantly during the twentieth century [11], and some of the recent extreme events were analyzed extensively (e.g., 2011 Western Australia [16], 2012 Northwest Atlantic [17], 2015–2016 Tasman Sea [18], 2016 Northern Australia, Gulf of Alaska and Bering Sea [19], and California Current [20]). The recent CMIP5 based ensemble analyses, relative to contemporary climatologies (e.g., 1960–1999, 1986–2005) [2, 21, 22] for example, predict more frequent and intensified marine heat events in response to anthropogenic climate change [5, 9], while local temperature anomalies could statistically depart from the current natural variability in the relatively near future [9, 23]. In addition, the latest IPCC report suggests that many ocean regions will continue to experience extreme events with greater normalcy [3].

The statistical analysis of past, present and future extreme events has primarily highlighted how background warming increases the intensity, frequency, and duration of extreme events. However, by contrast to these characterizations, we know little of how extreme events, especially those associated with warming, have evolved historically to become a new normal under global warming [11, 24]. This knowledge gap is problematic in part as it may lead to the false perception that marine ecosystems are primarily at risk in future time horizons, with less attention to the impacts of unprecedented heat extremes already being experienced on a global scale [11, 25, 26]. Furthermore, while these projection-based analyses are essential to climate adaptation efforts, substantial uncertainties and biases can arise due to the stochastic nature of global climate systems [27–30], further contributing to the lack of public consensus and action on climate change [31, 32].

Rigorous and transparent analyses of the dynamic marine environment with long-term records, however, can reliably characterize the emerging new normal marine climate in an appropriate historical context. Here, we use reconstructed climatological datasets providing a unique opportunity to explore the historical change in the occurrence of extreme marine heat events. Our analysis focused on sea surface temperature (SST), a key driver of marine ecosystems. We used 150 years of reconstructed SST datasets and analyzed changes in the frequency of historical marine heat extremes across all Exclusive Economic Zones, Biogeochemical Provinces, and Large Marine Ecosystems. With this analysis, we aim to describe the progression and expansion of extreme heat in global ocean and identify regions that have observed the most and least frequency of extreme heat. In doing so, our goal is to contextualize the present status of marine regions, indicating current climate disruptions and ecosystem risk, and to provide a timeline for the global ocean when historically benchmarked extreme events occurred more than 50%, thus becoming “normal.”

Methods

We used 150 years (1870–2019) of gridded, monthly reconstructed historical SST data sources to evaluate centennial changes in global occurrences of extreme marine heat events: the Hadley

Centre Sea Ice and SST dataset (HadISSTv1.1) [33] and the Characteristics of the Global SST data (COBESSTv2) [34] (Table A in S1 File). These independent and complementary global SST products were reconstructed from instrument records and the historical network of in situ measurements and have been widely deployed as ground-truthed SST fields [35, 36].

Our statistical definitions frame how we characterized the frequency and extent of extreme heat events across space and time. For each month, in each $1^\circ \times 1^\circ$ grid, we defined the extreme marine heat as a monthly average SST value that exceeds the 98th percentile SST value observed over 1870–1919 (corresponds to the period of second industrial revolution), or hottest temperature observed in the earliest 50-year period of record (Fig A in S1 File) [37–39]. Such percentile based thresholds can be derived from climatological data and are robust to drivers or variabilities associated with individual extreme events [10]. Our particular percentile based threshold also easily relates to the standard deviation (σ) which offers an alternative expression of dataset anomaly—the 98th percentile is when $\sigma = 2.05$. Though they are limited in describing daily and hourly extremes, we selected monthly SST products in order to evaluate the properties of extreme marine heat events at a $1^\circ \times 1^\circ$ scale within the longest historical context possible—150 years. At daily scales, species may respond to stressful abnormal temperatures by changing distributions but could suffer greater thermal-induced stress if an extreme heat event persists beyond one month. In addition, extreme heat events at shorter time scales are more likely to be smaller in scale than our analyzed spatial units (e.g., EEZs, large marine ecosystems). Furthermore, statistical analysis of monthly-resolved temperature variations can offer centennial-scale proxies of the frequency of extreme heat event properties [11].

A metric of the normalization of historical marine heat extreme event can be expressed as a fraction of a year that exceeds a locally identified threshold relative to the 1870–1919 climatology (hereafter referred to as a “local extreme heat index: LEHI”). For each grid cell, the LEHI is the proportion of each year (0–1) that exceeds the monthly extreme SST values. Threshold-based LEHI can quantify the magnitude and frequency of extreme events by summarizing the number of time units exceeding a fixed threshold at a given location. The LEHI can be further aggregated across space and time, offering a simple summary of heat extremes, or exceedance rates above the fixed historical benchmark for a season, period, or a region of interest. This proxy-based inference allowed us to generate global and centennial summaries of normalized extreme index from 1870 to 2019. If the climatology remains stationary throughout the full series, this value should approximate 0.02 independent of time or spatial scaling.

Having derived historical benchmarks of extreme heat, we generated summaries of a normalized LEHI for the global ocean from 1870–2019. For the global ocean, we mapped seasonal (Jan-Mar, Jul-Sep) LEHI summaries in recent decades (1980–2019) and calculated regional LEHIs for 2010–2019. We selected the regional frameworks of Large Marine Ecosystems [LMEs; 40], Exclusive Economic Zones [EEZs; 41], and biogeochemical provinces [BGCPs; 42] as they describe ecologically bounded transnational waters, political boundaries, and sub-basin scale perspectives on the distribution of marine heat extremes, respectively. To add to our understanding of centennial trends, we plotted the time series of changes in the fraction of surface area exceeding the historical 98th percentile threshold based on all calendar months for each of the seven major ocean basins (Table B in S1 File). Listed by descending area these are the: South Pacific (84.8×10^6 km²), North Pacific (77.0×10^6 km²), Indian (70.6×10^6 km²), North Atlantic (41.5×10^6 km²), South Atlantic (40.3×10^6 km²), Southern (22.0×10^6 km²), and Arctic (15.6×10^6 km²). For each basin, we calculated the year (if applicable) when 50% of the total area fraction exceeded and remained above the 1870–1919 climatology (i.e., the historical extreme heat benchmark, and referred to simply as climatology hereafter). The timing of such a thermal regime shift can be used to approximate the emergence of a new normal.

Further, our index ranks economically and ecologically important marine regions, identifying regions having the most and least risk of extreme heat.

Next, to highlight any different information presented in our approach, we compared the global variability of the LEHI to a more traditional SST anomaly metric. For the year 2019, we computed both spatial outputs from the same 1870–1919 climatology and the same spatial scale ($1^\circ \times 1^\circ$) to ensure that any differences are from the methodology alone. SST anomalies are widely used and an important impact parameter in climate extreme studies [10, 11, 21]. The difference in distributions of two climate indices derived from the same baseline period offers an alternative assessment of climate stress from the conventional anomaly-from-mean signals.

We conducted all data wrangling and analyses in the R programming environment [43], and provided our data and scripts in open access repositories (<https://bit.ly/2QjhYld>) and through the Open Science Framework (<https://osf.io/mj8u7/>).

Results

Fig 1 summarizes the decadal progression of global occurrences of extreme marine heat events from 1980–2019. In 2019 normalized extremes (LEHI > 0.5) occur broadly from the equatorial to the midlatitude regions in the Atlantic and Indian basins, stretching to the Norwegian and Barents, Philippine, and Tasman Seas. The global mean normalized LEHI increased significantly by 68.23% between the first and second half of this record (1980–1989 LEHI = 0.31, 2010–2019 LEHI = 0.52). By 2010–2019, many parts of the subtropical and midlatitude regions have reached a near-permanent extreme warming state. Throughout this record, extreme marine heat appears to advance from the far south Atlantic and Indian basins northward, with notable regions in the North Atlantic and South Pacific with a persistently low occurrence of heat extremes. The LEHI amplitude is greater during boreal summer (Jul-Sep) than boreal

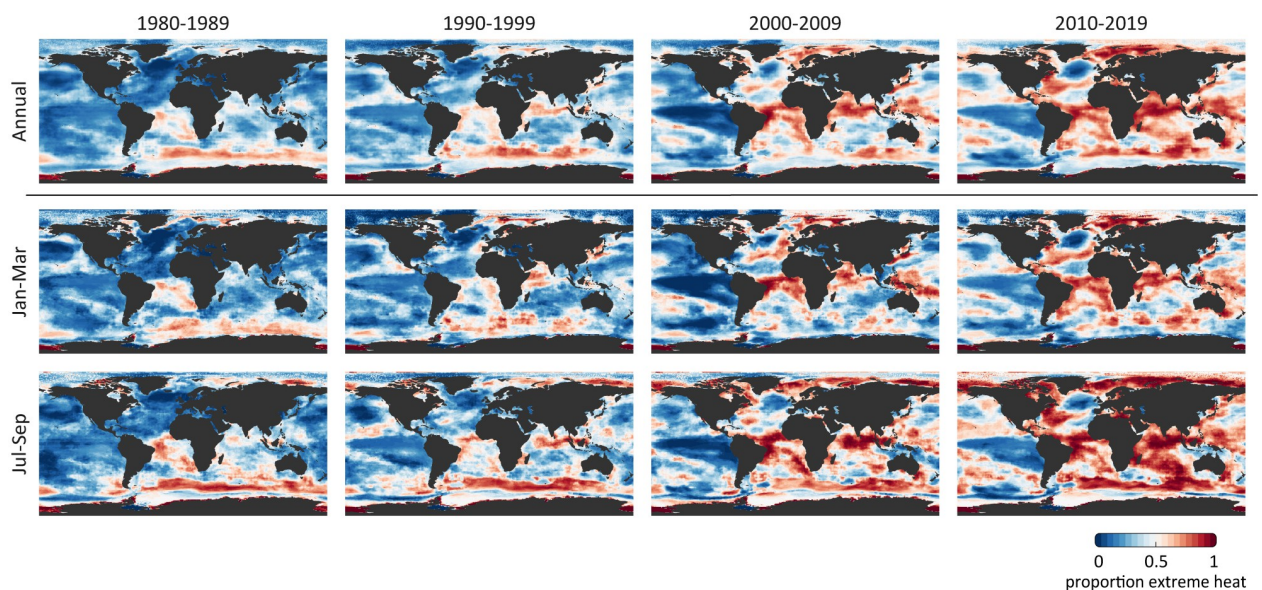


Fig 1. Decadal evolution of frequency of extreme marine heat from 1980–2019. Extreme heat defined as exceeding the localized ($1^\circ \times 1^\circ$), monthly, 98th percentile of sea surface temperatures (SST) observed during 1870–1919, averaged from HadISSTv1.1 and COBESSTv2 products. Extreme heat, resolved for boreal winter (Jan-Mar) and summer (Jul-Sep), accumulates steadily over time beginning in the Southern, South Atlantic, and Indian basins. Regions of the mid North Atlantic and eastern South Pacific indicate a low occurrence. The base map layer was drawn using the “rworldmap” R package (<https://cran.r-project.org/web/packages/rworldmap/index.html>; Accessed 6/27/2020).

<https://doi.org/10.1371/journal.pclm.0000007.g001>

winter (Jan-Mar) in both ocean hemispheres. HadISST and COBESST showed concurrence in the spatial distributions of LEHI (Fig B in S1 File), including the absence of normalizations in the Pacific South Equatorial Current and intersection of the Gulf Stream and Labrador Current. The largest seasonal difference occurred in the polar regions (Fig C in S1 File).

Contemporary summaries of LEHI from 2010–2019 highlight EEZs, LMEs, and BGCPs where current ocean climate stress is most pronounced (Fig 2). Regions that experienced a significant departure from climatology are not distributed evenly across the global ocean. Of the 142 EEZs, 66 LME, and 55 BGCPs examined, LEHI scores were highest between 35° N and 35° S, in the Tropic and Subtropic regions. Regions from the eastern Pacific Ocean with higher SST variability experienced relatively low LEHI values. The Maldives (median LEHI = 0.929) and Tanzania (0.925) both exhibited departure from climatology with a median value above 90% of the time, and 6 of the top 10 highest LEHI scores come from EEZs in the western Indian Ocean. The Somali Coastal Current and Scotian Shelf were two LMEs with the highest LEHI (0.889 and 0.873). Indian Monsoon Gyre was the only BGCP with a LEHI above 0.8 (0.808). The number of EEZs, LMEs, and BGCPs with LEHI in the upper tercile (>0.66) increased from none during 1980–1999 to 74 EEZs, 25 LMEs, and 15 BGCPs during 2010–2019 (Tables E-G in S1 File). Marine regions stretching across the western boundary of the American continents experienced the lowest increase in occurrence of extreme heat events.

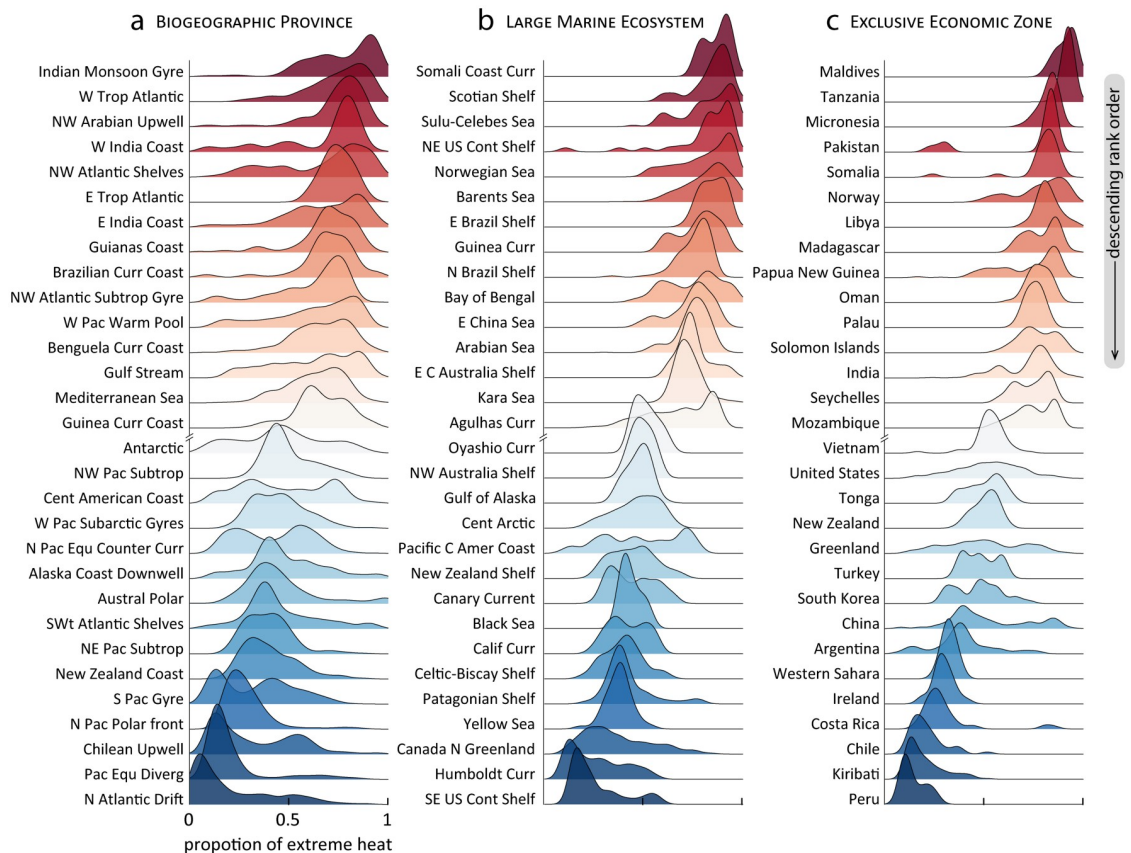


Fig 2. Regional variability of frequency of extreme marine heat during 2010–2019. Summaries for a, biogeochemical provinces b, Large marine ecosystems and c, Exclusive economic zones, displaying the outer 15 regions (30 total) from larger sets of 55, 66, and 142 regions, respectively. Regions are ranked and sorted by median extreme value. Tables E-G in S1 File present the unabridged series.

<https://doi.org/10.1371/journal.pclm.0000007.g002>

We find that from 1900 to 2019, the area fraction of global ocean surface exceeding the historical threshold (98th percentile during 1870–1919) exceeded 50% in 2014, while several major ocean basins outpaced the global average. Fig 3 shows an increase in the fraction of global and regional ocean surfaces exceeding the 1870–1919 extreme event threshold from less than 20% in the early 1900s to more than 50% in the 2010s. The period of 1980–2018 experienced a significant increase in global and regional area fractional exceedance, with strong El Niño events contributing to pronounced increases in 1998 and 2016. We define the point of no return (“PoNR”) as the year when more than 50% of surface areas exceeded and remained above the 1870–1919 threshold. This is first achieved in the South Atlantic (1998) and Indian

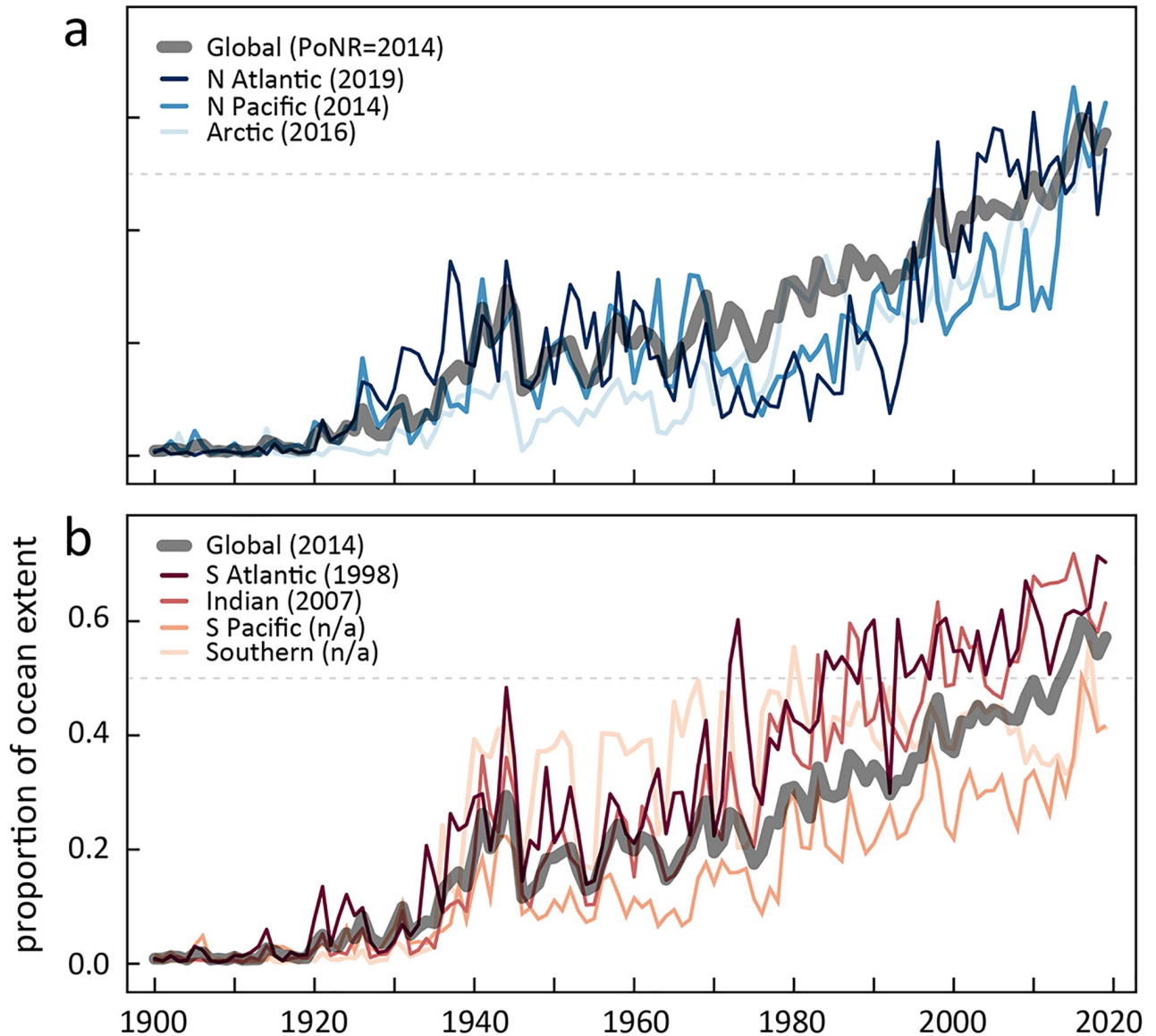


Fig 3. Synoptic frequency of extreme marine heat across ocean basins from 1900–2019. Fraction of the ocean surface annually experiencing extreme heat, grouped by **a**, northern hemisphere and **b**, southern hemisphere and Indian ocean basins. The Point of No Return (PoNR) occurs when each series surpasses and remains above 50% (dashed grey line), or when the historical baseline of extreme heat becomes ‘normal’. This first occurs in 1998 in the South Atlantic basin and for the global ocean occurs in 2014.

<https://doi.org/10.1371/journal.pclm.0000007.g003>

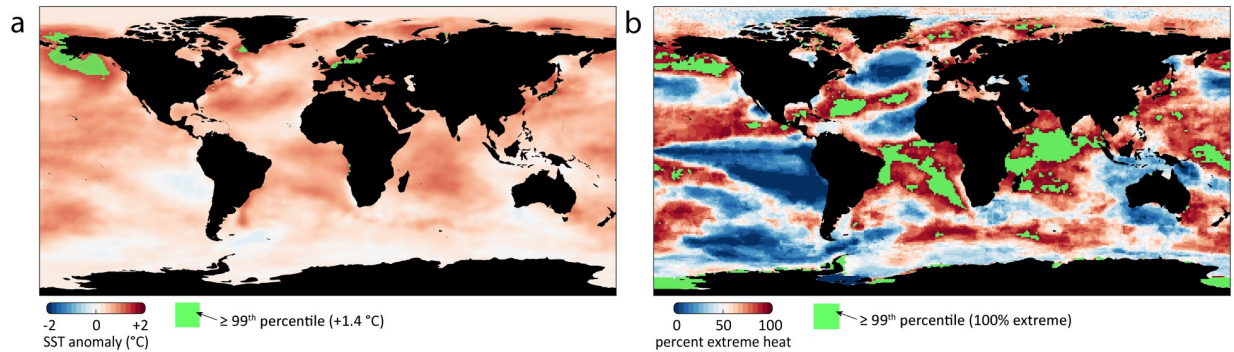


Fig 4. Comparing extreme marine heat metrics for the year 2019. **a**, Mean anomaly and **b**, percent extreme heat for the global ocean where both series have baselines determined from 1870–1919. Regions in the 99th percentile for each series (+1.4 °C and 100% extreme, respectively) are highlighted in green. This metric constitutes 7% of the global ocean in the extreme heat series, **b**, but only 1% for the more traditional mean anomaly approach, **a**. The base map layer was drawn using the “worldmap” R package (<https://cran.r-project.org/web/packages/rworldmap/index.html>; Accessed 6/27/2020).

<https://doi.org/10.1371/journal.pclm.0000007.g004>

(2007) basins, and occurs in 2014 for the entire global surface. Though, the Southern (1980, 2017) and South Pacific (2016) basins both surpass 50%, they subsequently drop below this value and therefore do not attain PoNR. We compared the mean area fraction of ocean surface exceeding the 1870–1919 extreme heat threshold between two time periods (1900–1959 and 1960–2019). The largest area fractional increase occurred in the Arctic (+533%) while the North Atlantic experienced the smallest fractional area increase (+147%) (Table C in [S1 File](#)).

The spatial distribution of normalized LEHI can be compared to the conventional climate indices derived from the IPCC-relevant climatology (1956–2005) in order to provide an alternative climate stress assessment at any point in time ([Fig 4](#)). Not unexpectedly, distributions of normalized LEHI and the SST anomalies have similarities and differences. According to the 2019 SST anomalies map, SST anomalies above 99 percentile (1.37 °C) were limited to the Chukchi Sea, Bering Sea, Gulf of Alaska Davis Strait, and southern portions of the North Sea and Baltic Sea, which *a priori* occurs in 1% of global ocean. However, the area of the global ocean with a normalized LEHI value above the 99th percentile (LEHI = 1) is substantially larger, covering 6.7% of global ocean.

Discussion

Regional drivers of LEHI

Spatial distributions of LEHI values may highlight regions with relatively small natural climate variability (narrower SST bounds; e.g., tropical Atlantic and tropical Indian Oceans; [\[44\]](#)). These regions generally exhibit relatively high signal-to-noise (S/N) ratios in observed data, where local warming exceeds observed interannual variability. Regions found to exhibit high S/N ratios are broadly aligned with our high LEHI values, especially in the tropics where climate signals have been emerged [\[44, 45\]](#). The similarity of LEHI values and S/N ratios are also clear in seasonal differences, with warmer months showing more significant changes [\[44\]](#). High LEHI values in the Northern Hemisphere also correspond to the Arctic-sea-ice boundary, where some of the strongest warming trends have been observed [\[46\]](#). On the other hand, low LEHI values (and low S/N ratios) are found in the equatorial Pacific region with high SST fluctuations dominated by ENSO processes [\[44, 46\]](#). Regional differences in LEHI values reflects (1) the strength of measured climate signals relative to the amplitude of local and regional variabilities and (2) show that the emergence of significantly different climates (i.e., normalization of extreme events) has already happened in many regions, particularly in the

low latitudes. These findings are consistent with recent studies that demonstrated the emergence of climate signals that would be unknown by past baselines were detectable at regional scales [44, 47, 48].

Added value from historically informed benchmarks

Knowledge of how local climate has varied in the past, relative to any historical baselines, is fundamental for understanding many aspects of the marine system in a changing climate. Studies on climate extremes has often addressed relatively recent trends or events in geographically restricted regions [49] or addressed present–future time horizons [9]. In the immediate aftermath of extreme events, there is often great public interest in attributing causes to extreme events soon after they occurred [50, 51]. However, researchers are increasingly recognizing the need to incorporate larger external forcings (e.g., atmospheric or oceanic circulation) for extreme event attributions at broader temporal scales. Detection of climate change impacts within a historical context offers clear advantages as reconstructed data are generally more reliable, especially during the period when global or near-global in situ data became available [52].

Using a statistical framework and globally reconstructed SST datasets, we demonstrate that many local climates have shifted out of their historical bounds. Our approach followed the statistical framework that is commonly used to examine the changes in the occurrence of univariate climate extreme events across time and space. This method that incorporates seasonally varying percentile thresholds with fixed or sliding baselines offers a suite of metrics that defines the characteristics of each event. For example, Oliver et al. [11] provided a global summary of the increase in annual MHW days, defined by a seasonally varying 90th percentile threshold based on a 1983–2012 climatology, along with other statistics including the duration and maximum intensity of each event. An advantage of our method is that it follows similar statistical definitions but provides a new metric that can be easily translated to the magnitude of climate normals, which can be calculated at any spatial and temporal scale.

Historical records can also provide new insights and empirical support to understand the role of non-equilibria dynamics and cumulative impacts of novel thermal disturbances that many regions have already incurred [53]. Understanding the full consequences of an individual extreme event is also best interpreted with substantial information from past disturbances [54]. While data from the longer past (e.g., before 1980) can be subject to larger uncertainties (e.g., sparser sampling and different measurement practices [12, 35], historical data can provide a wealth of information to understand interactions among sequences of climate-driven events if used with caution.

Extremes accounting provides an ecological reality check

Normalizing extreme marine heat events in a historical ecological context can be applied to evaluate the shifting baseline of ocean health and identify climate vulnerable regions. Large parts of the tropics are exhibiting clear emergence of warming signals [44]. Upwelling areas may moderate the severity and occurrence of extreme marine heat and therefore could function as ecological refugia for adjacent regions. Amplified normalization of extreme heat events in the Tropics suggests that biological hotspots in these regions have experienced unprecedented warming over the past decades. Major biodiversity hotspots in the Tropics include coral reef ecosystems that contain coral species that are close to their upper thermal tolerance. For habitat-forming organisms, relatively small increases of SST above the average summer maximum can lead to mass coral bleaching events, reduce seagrass density, and diminish kelp canopy coverage [26, 55]. The maintenance of this state or, worse, further increases in heat

extremes could potentially push many ecosystems beyond their thermal tolerance and towards permanent shifts.

While marine biota can typically adapt to gradual changes in environmental conditions [56–59], abrupt changes in the frequency and extent of extreme events experienced by local biodiversity can fundamentally alter the ecosystem structure, functions, and services [60]. Our results showed some of the largest LEHI values are found in the tropical Atlantic and tropical Indian Oceans (Fig 1). These changes in LEHI values may indicate the changes in the distribution of highly migratory species that are highly conditioned by water temperature. For example, our findings align with Monllor-Hurtado et al. [61], which showed the shift of tuna catches away from the tropics to the subtropics, likely reflecting the movement of tropical tuna populations to avoid these warmer thermal regimes in these regions.

Negative impacts of extreme marine heat events have been documented worldwide through extensive coral bleaching [62], mass mortality events [63], and toxic algal blooms [64]. Furthermore, a change in the frequency of extreme heat events in coastal waters, could be more harmful to sessile benthic species in the shallow water ecosystems [65] such as corals, kelps, and seagrasses. Further normalization of extremes could substantially impact the growth and reproduction of many commercial fisheries within LMEs and EEZs, with dramatic socioeconomic implications [21]. Improving our ability to connect past-present-future climate-driven ecological risks will allow us to develop a different set of management and conservation measures of living marine resources that better reflect spatially varying ocean health baselines [8, 9, 21].

Implications for climate science communication

Recent increases in extreme climatic events have heightened public discourse and concern over climate change impacts. At the same time, participants in climate change dialogues often express a strong interest in reliable information on historical and future changes as a basis for policies aimed at adaptation and planning. Simultaneously, characterization and assessment of extreme climatic events have become critically important criteria for a wide range of policy decisions. This study provides a robust historical framework to characterize extreme marine heat in order to inform climate change impacts at various spatial and temporal scales. Our globally resolved, centennial-scale extreme reanalysis can be used as a flexible and effective climate description and communication tool for the public and policymakers, and may help advance further science communication efforts to gain public understanding and confidence in extreme climate events and their attribution to anthropogenic climate change.

While the prediction of future climate change impacts remains challenging, facilitating constructive climate change dialogue may face fewer barriers when drawing from historical climate records. Using the methods applied here, we find that extreme climate change is not a hypothetical future possibility, but a past historical event that has already occurred in the global ocean. Though this occurred earlier in some regions, 50% of the ocean's surface experienced extreme heat in 2014, and this has steadily increased thereafter.

Supporting information

S1 File. Supplemental tables and figures are provided.
(DOCX)

Author Contributions

Conceptualization: Kisei R. Tanaka, Kyle S. Van Houtan.

Data curation: Kisei R. Tanaka, Kyle S. Van Houtan.

Formal analysis: Kisei R. Tanaka, Kyle S. Van Houtan.

Funding acquisition: Kisei R. Tanaka, Kyle S. Van Houtan.

Investigation: Kisei R. Tanaka, Kyle S. Van Houtan.

Methodology: Kisei R. Tanaka, Kyle S. Van Houtan.

Project administration: Kisei R. Tanaka, Kyle S. Van Houtan.

Resources: Kisei R. Tanaka, Kyle S. Van Houtan.

Software: Kisei R. Tanaka.

Supervision: Kisei R. Tanaka, Kyle S. Van Houtan.

Validation: Kisei R. Tanaka, Kyle S. Van Houtan.

Visualization: Kisei R. Tanaka, Kyle S. Van Houtan.

Writing – original draft: Kisei R. Tanaka, Kyle S. Van Houtan.

Writing – review & editing: Kisei R. Tanaka, Kyle S. Van Houtan.

References

1. Arguez A, Durre I, Applequist S, Vose RS, Squires MF, Yin X, et al. NOAA's 1981–2010 US climate normals: an overview. *Bulletin of the American Meteorological Society*. 2012; 93(11):1687–97.
2. IPCC. *Climate Change 2013: The Physical Science Basis. Contribution of Working Group I to the Fifth Assessment Report of the Intergovernmental Panel on Climate Change*. Cambridge, United Kingdom and New York, NY, USA: Cambridge University Press Cambridge; 2013.
3. IPCC. *IPCC Special Report on the Ocean and Cryosphere in a Changing Climate* 2019.
4. Katz RW. Statistics of extremes in climate change. *Climatic change*. 2010; 100(1):71–6.
5. Hayashida H, Matear RJ, Strutton PG, Zhang X. Insights into projected changes in marine heatwaves from a high-resolution ocean circulation model. *Nature communications*. 2020; 11(1):1–9.
6. Coumou D, Rahmstorf S. A decade of weather extremes. *Nature climate change*. 2012; 2(7):491–6.
7. Perkins S, Alexander L, Nairn J. Increasing frequency, intensity and duration of observed global heatwaves and warm spells. *Geophysical Research Letters*. 2012; 39(20).
8. Oliver EC, Burrows MT, Donat MG, Sen Gupta A, Alexander LV, Perkins-Kirkpatrick SE, et al. Projected marine heatwaves in the 21st century and the potential for ecological impact. *Frontiers in Marine Science*. 2019; 6:734.
9. Frölicher TL, Fischer EM, Gruber N. Marine heatwaves under global warming. *Nature*. 2018; 560(7718):360–4. <https://doi.org/10.1038/s41586-018-0383-9> PMID: 30111788
10. Hobday AJ, Alexander LV, Perkins SE, Smale DA, Straub SC, Oliver EC, et al. A hierarchical approach to defining marine heatwaves. *Progress in Oceanography*. 2016; 141:227–38.
11. Oliver EC, Donat MG, Burrows MT, Moore PJ, Smale DA, Alexander LV, et al. Longer and more frequent marine heatwaves over the past century. *Nature communications*. 2018; 9(1):1–12.
12. Schlegel RW, Oliver EC, Hobday AJ, Smit AJ. Detecting marine heatwaves with sub-optimal data. *Frontiers in Marine Science*. 2019; 6:737.
13. Chen K, Gawarkiewicz GG, Lentz SJ, Bane JM. Diagnosing the warming of the Northeastern US Coastal Ocean in 2012: A linkage between the atmospheric jet stream variability and ocean response. *Journal of Geophysical Research: Oceans*. 2014; 119(1):218–27.
14. Sparnocchia S, Schiano M, Picco P, Bozzano R, Cappelletti A, editors. *The anomalous warming of summer 2003 in the surface layer of the Central Ligurian Sea (Western Mediterranean)*. *Annales Geophysicae*; 2006: Copernicus GmbH.
15. Holbrook NJ, Scannell HA, Gupta AS, Benthuisen JA, Feng M, Oliver EC, et al. A global assessment of marine heatwaves and their drivers. *Nature Communications*. 2019; 10(1):1–13.
16. Wernberg T, Smale DA, Tuya F, Thomsen MS, Langlois TJ, De Bettignies T, et al. An extreme climatic event alters marine ecosystem structure in a global biodiversity hotspot. *Nature Climate Change*. 2013; 3(1):78–82.

17. Mills KE, Pershing AJ, Brown CJ, Chen Y, Chiang F-S, Holland DS, et al. Fisheries management in a changing climate: lessons from the 2012 ocean heat wave in the Northwest Atlantic. *Oceanography*. 2013; 26(2):191–5.
18. Oliver EC, Benthuisen JA, Bindoff NL, Hobday AJ, Holbrook NJ, Mundy CN, et al. The unprecedented 2015/16 Tasman Sea marine heatwave. *Nature communications*. 2017; 8(1):1–12.
19. Oliver EC, Perkins-Kirkpatrick SE, Holbrook NJ, Bindoff NL. Anthropogenic and natural influences on record 2016 marine heat waves. *Bulletin of the American Meteorological Society*. 2018; 99(1):S44–S8.
20. Jacox MG, Alexander MA, Mantua NJ, Scott JD, Hervieux G, Webb RS, et al. Forcing of multi-year extreme ocean temperatures that impacted California Current living marine resources in 2016. *Bull Amer Meteor Soc*. 2018; 99(1).
21. Alexander MA, Scott JD, Friedland KD, Mills KE, Nye JA, Pershing AJ, et al. Projected sea surface temperatures over the 21st century: Changes in the mean, variability and extremes for large marine ecosystem regions of Northern Oceans. *Elementa: Science of the Anthropocene*. 2018; 6(9).
22. Christidis N, Stott PA. Change in the odds of warm years and seasons due to anthropogenic influence on the climate. *Journal of Climate*. 2014; 27(7):2607–21.
23. Mora C, Frazier AG, Longman RJ, Dacks RS, Walton MM, Tong EJ, et al. The projected timing of climate departure from recent variability. *Nature*. 2013; 502(7470):183–7. <https://doi.org/10.1038/nature12540> PMID: 24108050
24. Oliver EC, Benthuisen JA, Darmaraki S, Donat MG, Hobday AJ, Holbrook NJ, et al. Marine heatwaves. *Annual Review of Marine Science*. 2021; 13:313–42. <https://doi.org/10.1146/annurev-marine-032720-095144> PMID: 32976730
25. Leiserowitz A. Communicating the risks of global warming: American risk perceptions, affective images, and interpretive communities. *Creating a climate for change: Communicating climate change and facilitating social change*. 2007:44–63.
26. Smale DA, Wernberg T, Oliver EC, Thomsen M, Harvey BP, Straub SC, et al. Marine heatwaves threaten global biodiversity and the provision of ecosystem services. *Nature Climate Change*. 2019; 9(4):306–12.
27. Sillmann J, Kharin V, Zhang X, Zwiers F, Bronaugh D. Climate extremes indices in the CMIP5 multimodel ensemble: Part 1. Model evaluation in the present climate. *Journal of Geophysical Research: Atmospheres*. 2013; 118(4):1716–33.
28. Kharin VV, Zwiers F, Zhang X, Wehner M. Changes in temperature and precipitation extremes in the CMIP5 ensemble. *Climatic change*. 2013; 119(2):345–57.
29. Schewe J, Gosling SN, Reyer C, Zhao F, Ciais P, Elliott J, et al. State-of-the-art global models underestimate impacts from climate extremes. *Nature communications*. 2019; 10(1):1–14.
30. Frank P. Propagation of Error and the Reliability of Global Air Temperature Projections. *Frontiers in Earth Science*. 2019; 7:223.
31. Schenck L. *Climate Change Crisis—Struggling for Worldwide Collective Action*. *Colo J Int'l Envtl L & Pol'y*. 2008; 19:319.
32. Van Houtan KS, Tanaka KR, Gagné T, Becker SL. The geographic disparity of greenhouse emissions and projected climate change. *Science Advances*. IN PRESS:1–9. <https://doi.org/10.1126/sciadv.abe4342> PMID: 34261645
33. Rayner N, Parker DE, Horton E, Folland CK, Alexander LV, Rowell D, et al. Global analyses of sea surface temperature, sea ice, and night marine air temperature since the late nineteenth century. *Journal of Geophysical Research: Atmospheres*. 2003; 108(D14).
34. Hirahara S, Ishii M, Fukuda Y. Centennial-scale sea surface temperature analysis and its uncertainty. *Journal of Climate*. 2014; 27(1):57–75.
35. Yasunaka S, Hanawa K. Intercomparison of historical sea surface temperature datasets. *International Journal of Climatology*. 2011; 31(7):1056–73.
36. Tommasi D, Stock CA, Alexander MA, Yang X, Rosati A, Vecchi GA. Multi-annual climate predictions for fisheries: An assessment of skill of sea surface temperature forecasts for large marine ecosystems. *Frontiers in Marine Science*. 2017; 4:201.
37. Barriopedro D, Fischer EM, Luterbacher J, Trigo RM, García-Herrera R. The hot summer of 2010: redrawing the temperature record map of Europe. *Science*. 2011; 332(6026):220–4. <https://doi.org/10.1126/science.1201224> PMID: 21415316
38. Hu K, Huang G, Zheng X-T, Xie S-P, Qu X, Du Y, et al. Interdecadal variations in ENSO influences on Northwest Pacific–East Asian early summertime climate simulated in CMIP5 models. *Journal of climate*. 2014; 27(15):5982–98.

39. Kent EC, Rayner NA, Berry DI, Eastman R, Grigorieva V, Huang B, et al. Observing requirements for long-term climate records at the ocean surface. *Frontiers in Marine Science*. 2019; 6:441.
40. Belkin IM. Rapid warming of large marine ecosystems. *Progress in Oceanography*. 2009; 81(1–4):207–13.
41. Flanders Marine Institute. Maritime Boundaries Geodatabase: Maritime Boundaries and Exclusive Economic Zones (200NM), version 11. <https://www.marineregions.org/>. 2019.
42. Reygondeau G, Longhurst A, Martinez E, Beaugrand G, Antoine D, Maury O. Dynamic biogeochemical provinces in the global ocean. *Global Biogeochemical Cycles*. 2013; 27(4):1046–58.
43. R_Core_Team. R: A language and environment for statistical computing. Vienna, Austria; 2019.
44. Hawkins E, Frame D, Harrington L, Joshi M, King A, Rojas M, et al. Observed emergence of the climate change signal: from the familiar to the unknown. *Geophysical Research Letters*. 2020; 47(6): e2019GL086259.
45. Hansen J, Fung I, Lacis A, Rind D, Lebedeff S, Ruedy R, et al. Global climate changes as forecast by Goddard Institute for Space Studies three-dimensional model. *Journal of geophysical research: Atmospheres*. 1988; 93(D8):9341–64.
46. Bulgin CE, Merchant CJ, Ferreira D. Tendencies, variability and persistence of sea surface temperature anomalies. *Scientific reports*. 2020; 10(1):1–13.
47. Mahlstein I, Knutti R, Solomon S, Portmann RW. Early onset of significant local warming in low latitude countries. *Environmental Research Letters*. 2011; 6(3):034009.
48. Mahlstein I, Hegerl G, Solomon S. Emerging local warming signals in observational data. *Geophysical Research Letters*. 2012; 39(21).
49. Lima FP, Wetthey DS. Three decades of high-resolution coastal sea surface temperatures reveal more than warming. *Nature communications*. 2012; 3(1):1–13. <https://doi.org/10.1038/ncomms1713> PMID: 22426225
50. Stott PA, Christidis N, Otto FE, Sun Y, Vanderlinden JP, van Oldenborgh GJ, et al. Attribution of extreme weather and climate-related events. *Wiley Interdisciplinary Reviews: Climate Change*. 2016; 7(1):23–41. <https://doi.org/10.1002/wcc.380> PMID: 26877771
51. Haustein K, Otto F, Uhe P, Schaller N, Allen M, Hermanson L, et al. Real-time extreme weather event attribution with forecast seasonal SSTs. *Environmental Research Letters*. 2016; 11(6):064006.
52. Hegerl GC, Brönnimann S, Cowan T, Friedman AR, Hawkins E, Iles C, et al. Causes of climate change over the historical record. *Environmental Research Letters*. 2019; 14(12):123006.
53. McClanahan TR, Maina JM, Darling ES, Guillaume MM, Muthiga NA, D'agata S, et al. Large geographic variability in the resistance of corals to thermal stress. *Global Ecology and Biogeography*. 2020; 29(12):2229–47.
54. Hughes TP, Kerry JT, Connolly SR, Baird AH, Eakin CM, Heron SF, et al. Ecological memory modifies the cumulative impact of recurrent climate extremes. *Nature Climate Change*. 2019; 9(1):40–3.
55. Hughes TP, Kerry JT, Baird AH, Connolly SR, Dietzel A, Eakin CM, et al. Global warming transforms coral reef assemblages. *Nature*. 2018; 556(7702):492–6. <https://doi.org/10.1038/s41586-018-0041-2> PMID: 29670282
56. Somero GN. Linking biogeography to physiology: evolutionary and acclimatory adjustments of thermal limits. *Frontiers in zoology*. 2005; 2(1):1. <https://doi.org/10.1186/1742-9994-2-1> PMID: 15679952
57. Walther G-R, Post E, Convey P, Menzel A, Parmesan C, Beebee TJ, et al. Ecological responses to recent climate change. *Nature*. 2002; 416(6879):389–95. <https://doi.org/10.1038/416389a> PMID: 11919621
58. Chevin L-M, Lande R, Mace GM. Adaptation, plasticity, and extinction in a changing environment: towards a predictive theory. *PLoS biology*. 2010; 8(4):e1000357. <https://doi.org/10.1371/journal.pbio.1000357> PMID: 20463950
59. Oostra V, Saastamoinen M, Zwaan BJ, Wheat CW. Strong phenotypic plasticity limits potential for evolutionary responses to climate change. *Nature communications*. 2018; 9(1):1–11.
60. Lough J, Anderson K, Hughes T. Increasing thermal stress for tropical coral reefs: 1871–2017. *Scientific reports*. 2018; 8(1):1–8.
61. Monllor-Hurtado A, Pennino MG, Sanchez-Lizaso JL. Shift in tuna catches due to ocean warming. *PloS one*. 2017; 12(6):e0178196. <https://doi.org/10.1371/journal.pone.0178196> PMID: 28591205
62. Eakin CM, Sweatman HP, Brainard RE. The 2014–2017 global-scale coral bleaching event: insights and impacts. *Coral Reefs*. 2019; 38(4):539–45.
63. Genin A, Levy L, Sharon G, Raitos DE, Diamant A. Rapid onsets of warming events trigger mass mortality of coral reef fish. *Proceedings of the National Academy of Sciences*. 2020. <https://doi.org/10.1073/pnas.2009748117> PMID: 32958634

64. Cavole LM, Demko AM, Diner RE, Giddings A, Koester I, Pagniello CM, et al. Biological impacts of the 2013–2015 warm-water anomaly in the Northeast Pacific: winners, losers, and the future. *Oceanography*. 2016; 29(2):273–85.
65. Galli G, Solidoro C, Lovato T. Marine heat waves hazard 3D maps and the risk for low motility organisms in a warming Mediterranean Sea. *Frontiers in Marine Science*. 2017; 4:136.